

A Distal, High-affinity Binding Site on the Cyclin-CDK Substrate Pho4 is Important for its Phosphorylation and Regulation

Meghan Byrne, Nicole Miller, Michael Springer and Erin K. O'Shea*

Department of Biochemistry
and Biophysics, Howard
Hughes Medical Institute
University of California, San
Francisco, 600 16th Street
Genentech Hall Room S472D
San Francisco, CA 94143-2240
USA

Cyclins and cyclin-dependent kinases (CDKs) are key components of signaling pathways essential for cell growth and survival. The cyclin-CDK Pho80-Pho85 inactivates the transcription factor Pho4 in budding yeast by phosphorylating it on five sites. We isolated seven single amino acid substitutions outside of the phosphorylation sites that cause Pho4 to be constitutively active. The substitutions decrease the amount of Pho4 phosphorylation *in vivo*, and they increase the apparent K_M of the *in vitro* phosphorylation reaction by an order of magnitude but do not alter k_{cat} substantially. These data suggest that the substituted residues are part of a cyclin-CDK-binding site that is distal to the phosphorylation sites. Further analysis revealed that all of Pho4 variants were phosphorylated by Pho80-Pho85 in a more distributive manner than the wild-type protein, further supporting the idea that binding at a distal, high-affinity binding site is important in determining the processivity of Pho4 phosphorylation. In addition, computational modeling of the Pho4 phosphorylation reactions shows that the K_D of binding between the Pho4 mutants and Pho80-Pho85 increases, confirming that the mutations are located in a relatively high-affinity "docking site" for the kinase. Interestingly, the K_D derived from the *in vitro* data correlates well with the strength of the *in vivo* phenotypes, demonstrating that the *in vitro* data are relevant to the *in vivo* regulation of Pho4.

© 2003 Elsevier Ltd. All rights reserved.

Keywords: cyclin-dependent kinase; transcription factor regulation; kinetic analysis; cyclin-binding domain; multi-site phosphorylation

*Corresponding author

Introduction

Cyclins and cyclin-dependent kinases (CDKs) control many important cellular processes including cell-cycle progression and metabolism.^{1,2} Cyclins are necessary for the activation of CDKs: cyclin binding causes a conformational change in the catalytic site that allows the CDK to position ATP and the substrate for phosphotransfer.³ Cyclins regulate the activity of CDKs by targeting them to correct substrates. This idea is supported by the observation that a single CDK, in complex

with different cyclins, can phosphorylate a different set of substrates.^{4,5}

While the targeting mechanisms are not fully understood, studies suggest that cyclin-CDKs recognize their substrates by binding to two different sites. One site is the phosphorylation site, for which the amino acid sequence S/TPXK/R (where the serine (S) or the threonine (T) is the phosphorylated residue and X is any amino acid) is common to most cyclin-CDK substrates.^{6,7} A crystal structure of cyclin A3-CDK2 in complex with a peptide containing the phosphorylation consensus sequence shows that this sequence binds the active site of the CDK and makes limited contact with the cyclin.³

The second site, which is less well understood, is distal to the phosphorylation sites and has a higher affinity for the cyclin-CDK than does the sequence containing the phosphorylation sites.^{3,8,9} The majority of distal binding sites identified thus far

Present address: N. Miller, Exelixis, Inc. 170 Harbor Way, PO Box 511, South San Francisco, CA 94083-0511, USA.

Abbreviations used: CDK, cyclin-dependent kinase; Pcl, Pho85-interacting cyclin; IEF, isoelectric focusing.

E-mail address of the corresponding author: oshea@biochem.ucsf.edu

contain the sequence arginine (R)-X-leucine (L), called the Cy motif.^{9–11} The presence of this distal binding site increases the efficiency of phosphorylation dramatically compared to non-physiological substrates that contain only a phosphorylation site, suggesting the distal binding site is important in increasing binding affinity between the substrate and the cyclin-CDK.^{10,12} Furthermore, the distal binding sites may help confer substrate specificity.¹³ One problem in trying to identify the role of distal, high-affinity binding sites in cyclin-CDK substrates is that few physiologically relevant substrates are known and, of those, few are biochemically tractable in their full-length form.

A physiologic substrate of the *Saccharomyces cerevisiae* cyclin-CDK complex Pho80-Pho85 is the transcription factor Pho4.¹⁴ Pho4 and Pho80-Pho85 are key regulators in the response of yeast to changes in the concentration of inorganic phosphate in the environment.¹⁵ In high-phosphate medium, Pho80-Pho85 phosphorylates and inactivates Pho4.¹⁴ In medium lacking phosphate, Pho80-Pho85 is inhibited by Pho81, a cyclin-dependent kinase inhibitor (CKI), leading to accumulation of unphosphorylated Pho4 and transcription of phosphate-responsive genes.^{16,17} Pho80-Pho85 phosphorylates Pho4 on five serine residues called SP1, SP2, SP3, SP4 and SP6, which conform to a consensus sequence SPXI/L.¹⁸ The phosphorylation sites play distinct roles in the regulation of Pho4 (Figure 1(a)).¹⁹ SP2 and SP3 phosphorylation increases the affinity of Pho4 for the nuclear transport receptor Msn5, which exports Pho4 from the nucleus. Phosphorylation on SP4, which is located within the nuclear-localization sequence of Pho4,²⁰ decreases the affinity of Pho4 for its nuclear import receptor, Pse1. Phosphorylation on SP6 decreases the affinity of Pho4 for its transcriptional co-activator Pho2, thereby preventing Pho4 from activating transcription of a subset of phosphate-responsive genes, including *PHO5*, which encodes a secreted acid phosphatase. SP1 is weakly phosphorylated and is not known to play a role in Pho4 regulation.^{18,19}

Much is understood about the mechanism of Pho4 phosphorylation by Pho80-Pho85 *in vitro*.²¹ Pho80-Pho85 phosphorylates SP6 preferentially; 50% of the time SP6 is the first site phosphorylated. In addition, Pho80-Pho85 phosphorylates Pho4 in a semi-processive manner in which a subset of the five sites is phosphorylated during each binding event. On average, 2.1 phosphorylation events occur before the kinase dissociates from the substrate. The semi-processivity of the reaction implies a binding interface that is separate from the phosphorylation sites. The distal site allows the kinase to remain bound while it exchanges ADP for ATP and phosphorylates multiple sites in a single binding event.

Several studies suggest that Pho80-Pho85 forms a high-affinity interaction with Pho4. An interaction between Pho80-Pho85 and Pho4 can be detected by co-immunoprecipitation, and this

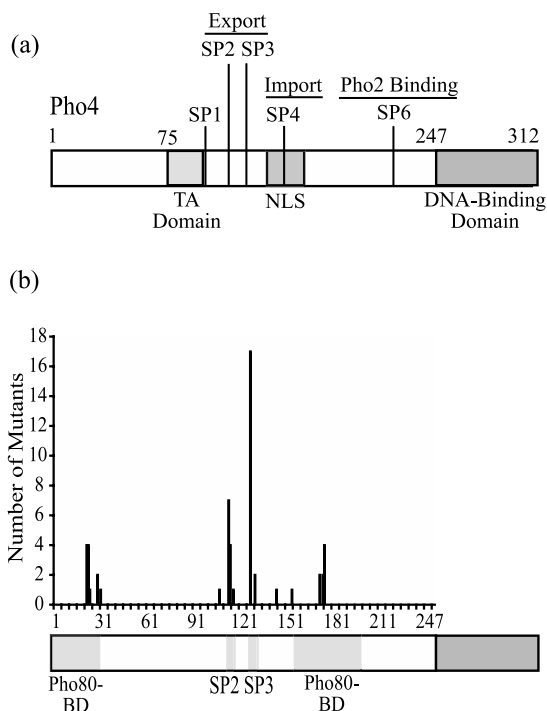


Figure 1. (a) Pho4 is phosphorylated on five serine-proline (SP) dipeptides (amino acid residues 100, 114, 128, 152, and 223).¹⁸ Phosphorylation on each of the sites plays a unique role in the regulation of Pho4.¹⁹ Phosphorylation of SP2 and SP3 promotes nuclear export. SP4 is located within the nuclear localization sequence (NLS) and its phosphorylation decreases nuclear import. Phosphorylation of SP6 decreases the binding affinity of Pho4 for the transcription factor Pho2. The transactivation (TA) domain is residues 75–99, the NLS is residues 140–166 and the DNA-binding domain is residues 247–312.^{25,39} (b) Constitutively-active Pho4 mutants isolated from PCR mutagenesis of the gene sequence encoding for amino acid residues 1–247 in *PHO4*^{PA6}. The distribution of amino acid substitutions was determined by counting the number of mutants containing mutations that occurred at least once as single residue substitutions. The majority of single-site mutations occurred in the two putative Pho80-binding domains (amino acid residues 1–30 and 156–200) and the SP2 and SP3 phosphorylation sites.²³ Tick marks occur every five amino acid residues.

interaction requires both Pho80 and Pho85.¹⁴ Pho85 in complex with other members of the family of Pho85-interacting cyclins (Pcls) cannot phosphorylate Pho4 as well, suggesting that Pho80-Pho85 binds with higher affinity to Pho4 than Pho85 in complex with other Pcls.²² Furthermore, synthetic peptides containing phosphorylation sites from Pho4 are phosphorylated much less efficiently than the full-length protein, suggesting a higher-affinity binding site exists outside the phosphorylation sites.²¹ Finally, yeast two-hybrid analysis has identified two regions of Pho4, distal to the phosphorylation sites, that are necessary and sufficient for interaction with Pho80.²³ Consistent with all previous data, single amino acid substitutions in Pho80 can suppress

the constitutive *PHO5* expression phenotype of a Pho4 mutant containing a substitution outside the phosphorylation sites, suggesting a direct interaction between the proteins.²⁴

In this study, we mutagenized the entire sequence of Pho4, excluding the DNA-binding domain, and performed a selection to identify residues of Pho4 that are part of the distal, high-affinity binding site. We identified seven residues that cluster in two different regions of primary sequence outside of the phosphorylation sites and showed that these residues are important for the phosphorylation of Pho4 both *in vitro* and *in vivo*. We show that all of the single amino acid substitutions decrease the processivity of the phosphorylation reaction *in vitro*. We also fit the *in vitro* data to a computational model of the Pho4 phosphorylation reaction. The K_D values derived from the modeling suggest that the affinity of the binding interaction between Pho80-Pho85 and the Pho4 mutants decreases compared to wild-type Pho4, supporting the hypothesis that the mutations are located in a distal, high-affinity binding site. The relative change in binding affinity is found to correlate well with the relative strength of the *in vivo* phenotype, supporting the relevance of the data acquired *in vitro* and the computational model.

Results

PCR mutagenesis and isolation of *PHO4^c* mutants

Because Pho80-Pho85 likely binds to Pho4 at a distal, high-affinity binding site, we wished to identify residues in Pho4, outside of the phosphorylation sites, that are important for its binding and phosphorylation by the Pho80-Pho85 complex. We performed a genetic selection for *PHO4^c* mutants that are constitutively active (*PHO4^c*) in a *PHO4* background where SP6 cannot be phosphorylated because the proline residue in SP6 is mutated to alanine (*PHO4^{PA6}*). Thus, Pho4^{PA6} is able to interact with Pho2 and activate *PHO5* transcription whenever it is localized to the nucleus. We utilized the *PHO4^{PA6}* background because it would likely reveal *PHO4* mutants with mild defects in phosphorylation. Three types of mutations could cause Pho4 to be constitutively active: a mutation in SP2 or SP3 that prevents phosphorylation of that site and therefore prevents nuclear export; a mutation that decreases binding affinity between Pho4 and Pho80, and leads to a decrease in phosphorylation; and a mutation outside SP2 and SP3 that prevents Msn5 binding and nuclear export. It is possible, though less likely, that Pho4 could acquire a gain-of-function mutation that would lead to an increase in binding between Pho4 and an activating phosphatase.

To select for *PHO4* mutants, PCR-mutagenized *PHO4^{PA6}* was introduced into a yeast strain carry-

ing the *HIS3* gene under the control of the *PHO5* promoter (*PHO5pr-HIS3*). In high-phosphate conditions, Pho4^{PA6} is cytoplasmic, preventing the expression of *PHO5* and *PHO5pr-HIS3* and causing the cells to be inviable on medium lacking histidine. However, Pho4 mutants that are constitutively active will activate transcription of *PHO5* and *PHO5pr-HIS3*, resulting in survival on medium lacking histidine and supplemented with 3-amino-1,2,4-triazole to increase the stringency of the selection for His3 activity.

We randomly chose 74 constitutively active Pho4 mutants for sequencing. Thirty-five mutants contained single amino acid changes and the remaining mutants contained multiple mutations. The most frequent mutations, which occurred at least once as a single amino acid substitution, were located either in the two putative Pho80-binding domains identified by two-hybrid analysis or in the SP2 and SP3 consensus phosphorylation site sequences (Figure 1(b)).²³ We did not pursue mutations in the phosphorylation sites because it is known that phosphorylation of both SP2 and SP3 is necessary for binding to Msn5 and export from the nucleus. Also, mutation of SP2 or SP3 does not affect phosphorylation of other sites, either *in vitro* or *in vivo* (data not shown). We chose the six most frequently occurring single amino acid substitutions outside the phosphorylation sites to investigate further (Table 1). Three cluster in the N-terminal putative Pho80-binding domain (an isoleucine to threonine substitution at residue 22 (I22T), a leucine to histidine substitution at residue 23 (L23H), and a phenylalanine to isoleucine substitution at residue 29 (F29I)). The other three cluster in the C-terminal putative Pho80-binding domain (a leucine to serine substitution at residue 173 (L173S), an aspartic acid to valine substitution at residue 175 (D175V), and a serine to asparagine substitution at residue 176 (S176N)). We included a proline to leucine substitution at residue 174 (P174L), since it had been identified as a constitutively-active Pho4 mutant and lies in the C-terminal domain.²⁵

These seven residues were identified in another selection for constitutively active Pho4 mutants. In

Table 1. Results from *PHO4^c* mutant selection

Residues ^a	Substitutions	Number of mutants	Mutation followed
I22	T	4	I22T
L23	H,P	4	L23H
F29	I,V,S	3	F29I
L173	S	2	L173S
D175	V,Y	2	D175V
S176	N,Y	4	S176N
SP2 Site (SPLI)	-	8	ND ^b
SP3 Site (SPNL)	-	19	ND

^a These residues were mutated the most frequently in mutants with single-site amino acid substitutions.

^b ND = not done.

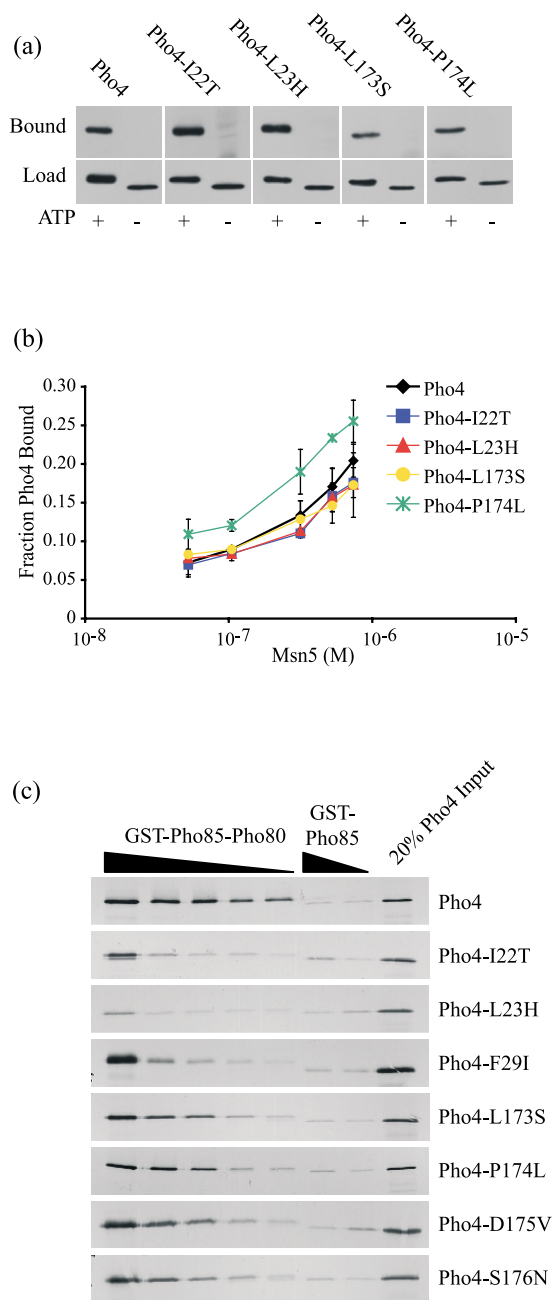


Figure 2. The Pho4^C mutants are not defective in binding Msn5 but do show a decrease in binding Pho80-Pho85. (a) Phosphorylated but not unphosphorylated Pho4 binds Msn5. Wild-type Pho4 and four Pho4 mutants were either phosphorylated (+ATP) or mock phosphorylated (-ATP) and incubated with Msn5 and zz-tagged RanGTP immobilized on IgG-Sepharose. Bound proteins were separated by SDS-PAGE, and Pho4 was visualized by Western blotting with a Pho4 antibody. (b) Wild-type Pho4 and the Pho4 mutants were phosphorylated and labeled with ³²P *in vitro*, then incubated with Msn5 and zz-tagged RanGTP bound to IgG-Sepharose beads. The amount of bound Pho4 was determined as a fraction of Pho4 added to the binding reaction. Wild-type Pho4 and the Pho4 mutants were analyzed by isoelectric focusing to confirm they were phosphorylated to completion (data not shown). (c) The Pho4 mutants show a range of decreased binding to GST-Pho85-Pho80 compared to wild-type Pho4. Wild-type Pho4 and the Pho4 mutants were labeled with

this selection, wild-type *PHO4* was used as the template for mutagenesis (E. M. O'Neill, A. Komeili & E.K.O'S., unpublished results). This suggests that the *PHO4*^C mutants do not require a mutation in SP6 to be constitutively active. For all subsequent experiments, we studied the mutations in the context of Pho4 containing wild-type SP6.

The Pho4^C mutants localize to the nucleus in cells grown in high-phosphate medium

We subcloned each of the *PHO4* mutations into a low-copy vector containing *PHO4* tagged with *GFP* and examined the localization of the resulting proteins in high-phosphate medium. As expected, the constitutively active Pho4 mutants localized to the nucleus in high-phosphate medium. This localization is similar to wild-type Pho4-GFP in phosphate-free medium, where Pho4 is active, and in a *pho80Δ* yeast strain in high-phosphate medium, where Pho4 cannot be phosphorylated (data not shown). These results indicate that the Pho4 mutations impair Pho4 nuclear export. This defect could result from a decrease in phosphorylation of SP2 and/or SP3, which would decrease the binding of Pho4 and Msn5, or from a mutation in the Msn5-Pho4 binding interface, outside the phosphorylation sites.

The Pho4 mutants are able to bind Msn5 but are defective in binding Pho80-Pho85 *in vitro*

To address the possibility that the Pho4^C mutants have a defect in binding Msn5 even if they are phosphorylated on SP2 and SP3, we performed *in vitro* binding assays with Msn5, RanGTP, and recombinant, purified Pho4 that was mock-phosphorylated or phosphorylated to completion (Figure 2(a) and (b)). RanGTP is necessary for cooperative binding with Msn5 and Pho4.^{26,27} We chose four Pho4 mutants, two having mutations in the N-terminal region and two in the C-terminal region, and examined the binding of these mutants to Msn5 at five concentrations of Msn5. Binding of the Pho4 mutants to Msn5-RanGTP was still phosphorylation-dependent and was unchanged compared to wild-type Pho4, suggesting strongly that the mutations do not cause a defect in binding Msn5.

To determine if the Pho4^C mutations affect the interaction of Pho4 with Pho80-Pho85, we performed an *in vitro* pull-down assay with unphosphorylated Pho4 and Pho80-Pho85 tagged with GST (Figure 2(c)). The Pho4^C mutants showed decreased binding to GST-Pho85-Pho80 compared

[³⁵S]methionine and 0.2 nM Pho4 was incubated with 400, 62.5, 25, 10, or 4 nM GST-Pho85-Pho80 immobilized on glutathione-agarose. After extensive washing, bound Pho4 was analyzed by SDS-PAGE. GST-Pho85 at 400 nM and 4 nM was used as a negative binding control.

to wild-type Pho4, across five concentrations of GST-Pho85-Pho80. These results suggest that the constitutive activity of the Pho4 mutants may be due to a decrease in binding affinity with the kinase, leading to a decrease in phosphorylation. We did not determine binding affinities from this assay because binding of Pho4 was never saturated, and dimerization of GST could likely affect the binding behavior.

Phosphorylation of the Pho4^C mutants is reduced *in vitro*

To investigate the hypothesis that Pho80-Pho85 is not able to phosphorylate the Pho4 mutants as well as wild-type Pho4, we performed *in vitro* kinase assays with Pho4 and Pho80-Pho85-His₆ purified from *Escherichia coli*. The rate of molar phosphate transfer was determined at a substrate concentration approximately threefold higher than the K_M for phosphorylation of wild-type Pho4 by Pho80-Pho85.²¹ At this concentration, the rate of phosphorylation of the Pho4 mutants by Pho80-Pho85 was significantly slower than that of wild-type Pho4 (Figure 3). Therefore, the Pho4 mutants are defective in phosphorylation *in vitro*, and this defect likely results from impaired interaction with Pho80-Pho85.

Characterization of the *in vivo* phenotypes

To characterize the *PHO4^C* mutant phenotypes *in vivo*, we determined quantitatively the activity of the *PHO* pathway in yeast strains expressing the Pho4 mutants by performing acid phosphatase assays on yeast cultures grown in phosphate-free and high-phosphate media. These phosphatase assays measure the activity of Pho5, a secreted acid phosphatase whose transcription is activated by Pho4 when cells are starved for phosphate. In high-phosphate medium, cells containing the *PHO4^C* mutants had more phosphatase activity

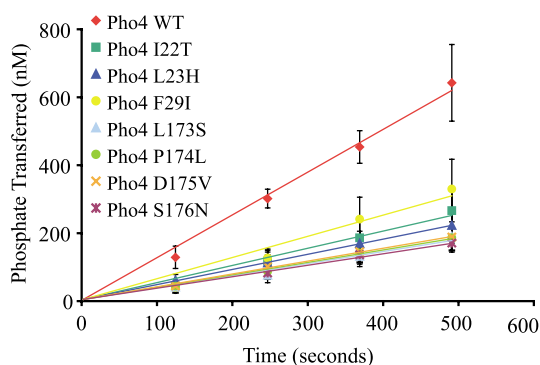


Figure 3. Pho80-Pho85 phosphorylates the Pho4 mutants at a slower rate than wild-type Pho4. The amount of phosphate transferred to 1 μ M wild-type or mutant Pho4 was determined at four time-points following the addition of 0.1 nM Pho80-Pho85. The Pho4 mutants and wild-type Pho4 were at a concentration approximately three times the K_M of wild-type Pho4.

than cells containing wild-type *PHO4*, confirming that the *PHO4^C* mutants cannot be inactivated completely in conditions where the pathway is normally off (Figure 4(a)). Cells containing different *PHO4^C* mutants produced different levels of phosphatase activity. For instance, *PHO4-D175V* had a twofold increase in phosphatase activity compared to wild-type *PHO4*, whereas *PHO4-P174L* showed an almost fivefold increase. After being starved for phosphate for three hours, cells containing the Pho4 mutants had higher levels of phosphatase activity than in high-phosphate medium, showing that they can still be somewhat regulated in response to extracellular phosphate levels.

Since the mutants cluster in two regions of primary sequence in the Pho4 protein, we decided to combine two amino acid substitutions, one from each region, and determine if the double mutant has a stronger phenotype. Interestingly, the double mutant, *PHO4-L23H,P174L*, showed a complete lack of regulation. The levels of phosphatase activity in cells containing the double mutant were similar to the levels in a *pho80* Δ strain, where there is no kinase activity and Pho4 is unphosphorylated.

Phosphorylation of the Pho4^C mutants is reduced *in vivo*

To investigate if the *PHO4^C* mutants are defective in phosphorylation *in vivo*, we examined the phosphorylation of the Pho4 mutant proteins in whole-cell yeast extracts. Yeast extracts were made from cells containing wild-type or mutant *PHO4* grown in high-phosphate medium and examined by Western blotting with antibodies recognizing full-length Pho4 or phosphopeptide-specific antibodies recognizing phosphorylated SP2, SP3, or SP6. The signal from the full-length Pho4 antibody was used to control for differences in loading, and the amount of phosphorylation of each Pho4 mutant was normalized to the phosphorylation of wild-type Pho4 (Figure 4(b)). All of the Pho4 mutants were less phosphorylated on SP2, SP3, and SP6 than wild-type Pho4. The double mutant was the least phosphorylated, having levels of phosphorylation close to background, as determined in the *pho80* Δ strain, which lacks Pho80-Pho85 kinase activity. These results support the hypothesis that the mutated residues are important for the phosphorylation of Pho4 *in vivo*.

Kinetic analysis of *in vitro* phosphorylation

To investigate how the Pho4^C mutations affect the kinetics of phosphorylation, we extended the *in vitro* kinase assays to determine the specific activity of Pho80-Pho85 for wild-type Pho4 and the Pho4 mutants. We used Henri-Michaelis-Menten kinetic analysis to calculate the apparent k_{cat} and K_M for each of the phosphorylation reactions. Because there are five phosphorylation sites,

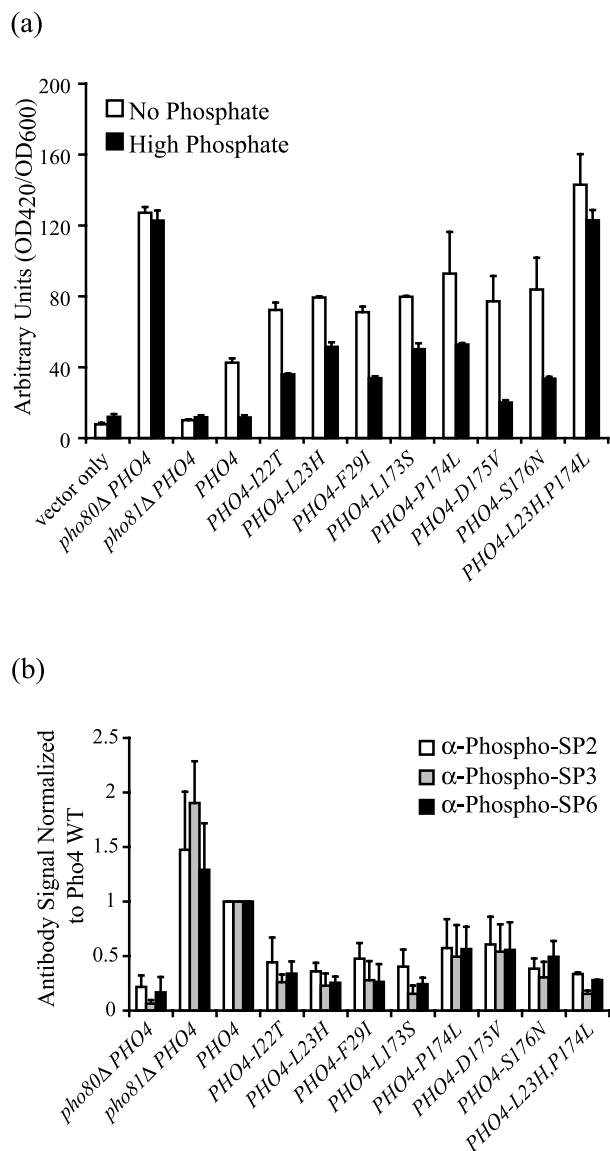


Figure 4. Characterization of *PHO4^C* mutant phenotypes and phosphorylation *in vivo*. (a) Strains containing single-site *PHO4* mutants have increased Pho5 phosphatase activity compared to a wild-type *PHO4* strain grown in high-phosphate medium, and the levels of phosphatase activity increase further when the cells are starved for phosphate. A strain containing a *PHO4* double mutant shows maximal levels of phosphatase activity in both high-phosphate and phosphate-free media. In *pho80Δ* cells, Pho4 cannot be phosphorylated and is always active. In *pho81Δ* cells, Pho80-Pho85 is constitutively active, so Pho4 is phosphorylated and inactive, regardless of phosphate levels. *pho4Δ* (EY0130), *pho4Δ pho80Δ* (EY0219), and *pho4Δ pho81Δ* (EY0270) cells were transformed with p*PHO4*_{pr}-*PHO4*. *pho4Δ* (EY0130) cells were transformed with YCp50 and YCp50-based plasmids expressing each of the *PHO4^C* mutants. (b) The *PHO4^C* mutants are defective in phosphorylation *in vivo*. Whole-cell extracts were made from cells containing wild-type or mutant Pho4 grown in high-phosphate medium. Levels of Pho4 and Pho4 phosphorylation were analyzed by Western blotting analysis with anti-Pho4 polyclonal antibody or antibody specific to phosphorylated SP2, SP3, or SP6. Levels of Pho4 phosphorylation were determined by quantifying the level of

this standard kinetic analysis cannot determine the true k_{cat} and K_M . Instead, it gives an apparent k_{cat} and K_M that are composite values for the phosphorylation of all five sites.²¹ The apparent K_M values for the Pho4 mutants were one order of magnitude greater than the apparent K_M for wild-type Pho4, while the apparent k_{cat} values for the Pho4 mutants were similar to the apparent k_{cat} of wild-type Pho4 (Table 2). The fact that the apparent K_M is one order of magnitude greater for phosphorylation of the mutants suggests that the mutations decrease the affinity of the kinase for the substrate without disrupting binding completely. While we cannot determine the exact change in the binding affinity from the K_M , since it is affected by the k_{cat} , it can give us an idea of the change. For comparison, the K_M for phosphorylating peptides containing SP2, SP4, or SP6 is 1000-fold greater than the apparent K_M for the phosphorylation of wild-type Pho4, while the k_{cat} values for peptide phosphorylation are similar to the apparent k_{cat} for wild-type Pho4.²¹ These data suggest that the difference in K_M is due to the presence of a distal, high-affinity binding site in the full-length protein.

We investigated whether the Pho4 mutations affect the semi-processivity of the phosphorylation reaction. Pho80-Pho85 phosphorylates wild-type Pho4 on a subset of the five phosphorylation sites each time the kinase binds the substrate.²¹ We reasoned that if the mutations decrease the binding affinity at the distal binding site, as hypothesized, it is likely that they affect the number of times that Pho80-Pho85 phosphorylates Pho4 before dissociating. We performed an *in vitro* kinase reaction followed by one-dimensional isoelectric focusing (IEF) to separate the different phosphoforms of Pho4 and determined their relative abundance. In the kinase reaction, we added Pho4 in excess over the kinase (6 μ M and 0.1 nM, respectively) to decrease the likelihood that the kinase will bind and phosphorylate Pho4 that has already been phosphorylated. During a 30 minute reaction, the relative amounts of the five phosphoforms did not change, supporting the idea that phosphorylated molecules of Pho4 are not rephosphorylated in this time (data not shown).

The Pho4 mutants were phosphorylated fewer times per binding event than wild-type Pho4, as seen by the relative increase in phosphoform 1 and decrease in the four higher phosphoforms (Figure 5). We calculated the average number of phosphorylation events per binding event and found that the Pho4 mutants were phosphorylated

antibody signal using a CCD camera (Alpha Innotech). Signal from the phosphopeptide-specific antibodies was normalized to the amount of phosphorylation of wild-type Pho4. Differences in loading of samples were corrected by dividing each phosphopeptide-specific antibody signal by the Pho4 antibody signal.

Table 2. Kinetic constants for Pho4 wild-type and Pho4^C mutants

Molecule	K_M (μM) ^a	k_{cat} (s^{-1}) ^a
Pho4	0.3–0.4	10–14
Pho4-I22T	2–4	11–17
Pho4-L23H	3.5–4	21–24
Pho4-F29I	2.5–3.5	14–14.5
Pho4-L173S	5–5.5	9–13
Pho4-P174L	1.5–2	9–14
Pho4-D175V	3–3.5	15–17
Pho4-S176N	2.5–4	12–20
Pho4-L23H,P174L	3–6	10–17

These are apparent kinetic constants since they describe the phosphorylation of five sites on each Pho4 monomer.

^a Assays to determine the apparent K_M and k_{cat} were repeated two or more times. The kinetic constants are reported as the range of values obtained.

between 1.2 and 1.5 times per binding event, whereas wild-type Pho4 is phosphorylated 2.1 times per binding event. Thus, all the Pho4 mutants were phosphorylated more distributively than wild-type Pho4. These results support the idea that the mutations change the balance between the dissociation rate at the distal site and the phosphotransfer rate, which determines how many times the substrate is phosphorylated in a single binding event.

To determine whether the Pho4 mutations

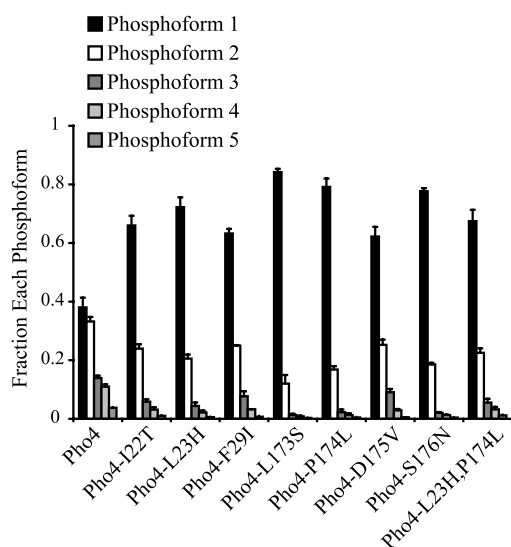


Figure 5. The Pho4 mutants are phosphorylated less processively than wild-type Pho4. Pho80-Pho85 (0.1 nM) was added to excess Pho4 (6 μM) to increase the likelihood that a molecule of Pho80-Pho85 would phosphorylate an unphosphorylated molecule of Pho4 during the experiment. The reaction was stopped at various times and the sample run on isoelectric focusing gels to separate the Pho4 phosphoforms. The amount of each phosphoform was quantified and expressed as a fraction of total phosphorylated Pho4. An increased fraction of the lower phosphoforms indicates that phosphorylation is less processive.

change the site preference of the kinase for phosphorylating SP6 before the other phosphorylation sites, we performed tryptic phosphopeptide mapping on the phosphoforms from one mutant with a mutation in the N-terminal Pho80-binding region (Pho4-L23H) and two with mutations in the C-terminal Pho80-binding region (Pho4-L173S and Pho4-P174L). None of the three mutants showed a significant change in site preference compared to wild-type Pho4 (data not shown), suggesting that these mutations do not alter the relative rates of phosphorylation of each site, just the overall rate.

Computational modeling of the *in vitro* phosphorylation data

To obtain values for the change in binding affinity between the Pho4 mutants and Pho80-Pho85, we turned to a computational model of the Pho4 phosphorylation reaction that has been published.²¹ We fit the model to data from *in vitro* phosphorylation experiments to determine k_{on} and k_{off} values for Pho80-Pho85 binding to Pho4 and k_{cat} values for phosphorylation of each SP site. Specifically, the variables were constrained by three sets of experimental data: the kinetic analysis used to determine the apparent k_{cat} and K_M , the processivity of phosphorylation, and the site preference in phosphoforms 1–4. We assumed that the kinase has the same SP site preference when phosphorylating the mutants as it does for wild-type Pho4, which we felt was a reasonable assumption, since the site preference is unchanged for three of the mutants (see above). We used a multi-variable, random-walk search and least-squares analysis to find the best-fitting values and were able to obtain 95% confidence intervals for wild-type Pho4 and all the Pho4^C mutants (Figure 6(a) and (b)).

The model predicts that the k_{on} for Pho80-Pho85 binding Pho4 decreases and the k_{off} for the unphosphorylated form of Pho4 increases for the majority of the mutants (Table 3). The k_{cat} for the first phosphotransfer event on Pho4 remains unchanged or decreases compared to wild-type Pho4. From the k_{on} and k_{off} values, we calculated the predicted K_D . The model predicts that the K_D increases for all the mutants between two- and tenfold compared to the wild-type Pho4 interaction with Pho80-Pho85. These results support the hypothesis that the mutations decrease the binding affinity between Pho4 and Pho80-Pho85 at the distal binding site. Also, the k_{cat} values for the Pho4 mutants are closer to the experimentally measured k_{cat} values than for wild-type Pho4, supporting the idea that the phosphorylation reaction is less processive and that the k_{cat} for the mutants is not limited by k_{off} as much as k_{cat} for wild-type Pho4.

To investigate how well the change in kinetic constants from the model matches the *in vivo* phenotypes of the mutants, we asked how well the Pho5 activity in wild-type and mutant strains grown in high-phosphate medium is predicted by

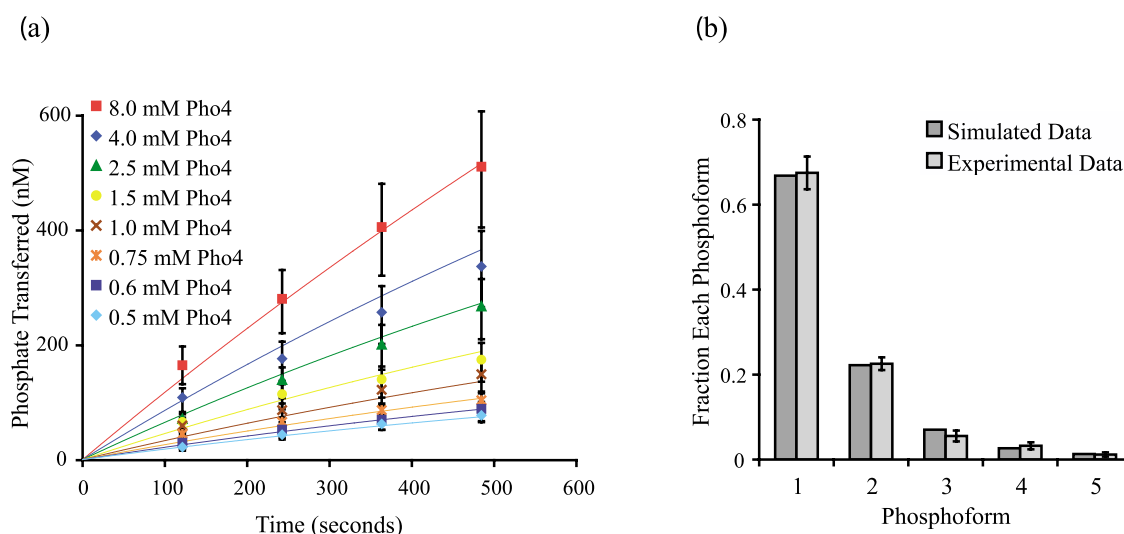


Figure 6. Fit of the computational model to the experimental data from Pho4-L23H,P174L. (a) Simulation of the apparent k_{cat}/K_M data by the computational model. The points represent the concentration of phosphate transferred to Pho4 at different times and at different concentrations of Pho4. The error bars represent the standard deviation from three independent experiments and are within 20% of the average. The lines are the values produced from a simulation of the experiment based on the computational model. Similar fits were obtained for wild-type Pho4 and the other seven Pho4 mutants. (b) Simulation of the early distribution of phosphoforms when Pho4 (6 μM) is in large excess of Pho80-Pho85 (0.1 nM). The bars represent the fraction of Pho4 phosphorylated one, two, three, four or five times. Similar fits were obtained for wild-type Pho4 and the other seven Pho4 mutants.

various kinetic parameters. Strikingly, Pho5 activity *in vivo* is correlated closely to K_D (R squared value, 0.94) (Figures 4(a) and 7(a)). The K_D values used in the plot are for binding between Pho80-Pho85 and the unphosphorylated Pho4 proteins. Although the K_D changes as Pho4 is phosphorylated, the change is relatively small and is a similar magnitude for wild-type Pho4 and all the mutants (data not shown).²¹ The correlation between binding affinity and relative levels of Pho5 activity suggests that the binding affinity at the distal binding site is an important factor in the efficiency of phosphorylation *in vivo*. In contrast, the k_{cat} or rate of phosphotransfer once Pho80-Pho85 is bound to Pho4, does not correlate with the *in vivo* levels of Pho5 activity (Figure 7(b)). Also, the number of times Pho4 is phosphorylated in a single binding event and the apparent K_M , which gives the substrate concentration at which the overall rate of phosphorylation is half maximal,

do not correlate well with Pho5 activity *in vivo* (Figure 7(c) and (d)).

Discussion

We have identified seven residues in Pho4, distal to the actual phosphorylation sites, that are important for its phosphorylation both *in vivo* and *in vitro*. These residues are located in two regions of Pho4 that were identified as putative Pho80-binding domains in a yeast two-hybrid analysis.²³ Our data suggest that this interaction allows the kinase to bind Pho4 with high affinity at a site distal to the phosphorylation sites and to phosphorylate multiple sites prior to dissociating.

We characterized seven amino acid substitutions in the two Pho80-binding domains that occurred the most frequently in our selection for constitutively active Pho4 mutants. All seven substitutions

Table 3. Kinetic constants derived from computational modeling of the *in vitro* Pho4 phosphorylation reaction

	k_{on} ($\text{M}^{-1} \text{s}^{-1}$) $\times 10^7$	k_{off} (s^{-1})	k_{cat} (s^{-1})	K_D (μM) ^a
Pho4	2.2–2.4	8.9–10.0	26.0–28.0	0.37–0.46
Pho4-I22T	0.9–1.1	21.1–25.5	16.5–21	1.9–3.0
Pho4-L23H	1.0–1.3	32.6–42.1	21.0–25.3	2.6–4.3
Pho4-F29I	1.2–1.4	21.2–29.6	17.5–22.8	1.5–2.5
Pho4-LI73S	1.1–1.4	29.7–37.8	9.3–11.8	2.1–3.4
Pho4-P174L	1.3–2.2	36.3–42.4	13.2–19.1	1.7–3.3
Pho4-D175V	2.0–2.5	20.0–26.5	15.8–18.4	0.79–1.4
Pho4-S176N	2.1–2.3	41.8–43.4	23.6–25.7	1.8–2.1
Pho4-L23H,P174L	0.6–0.7	33.2–39.3	20.4–26.4	4.6–6.7

All constants are for binding and phosphorylation of Pho4 that is unphosphorylated.

^a Calculated from k_{off} and k_{on} .

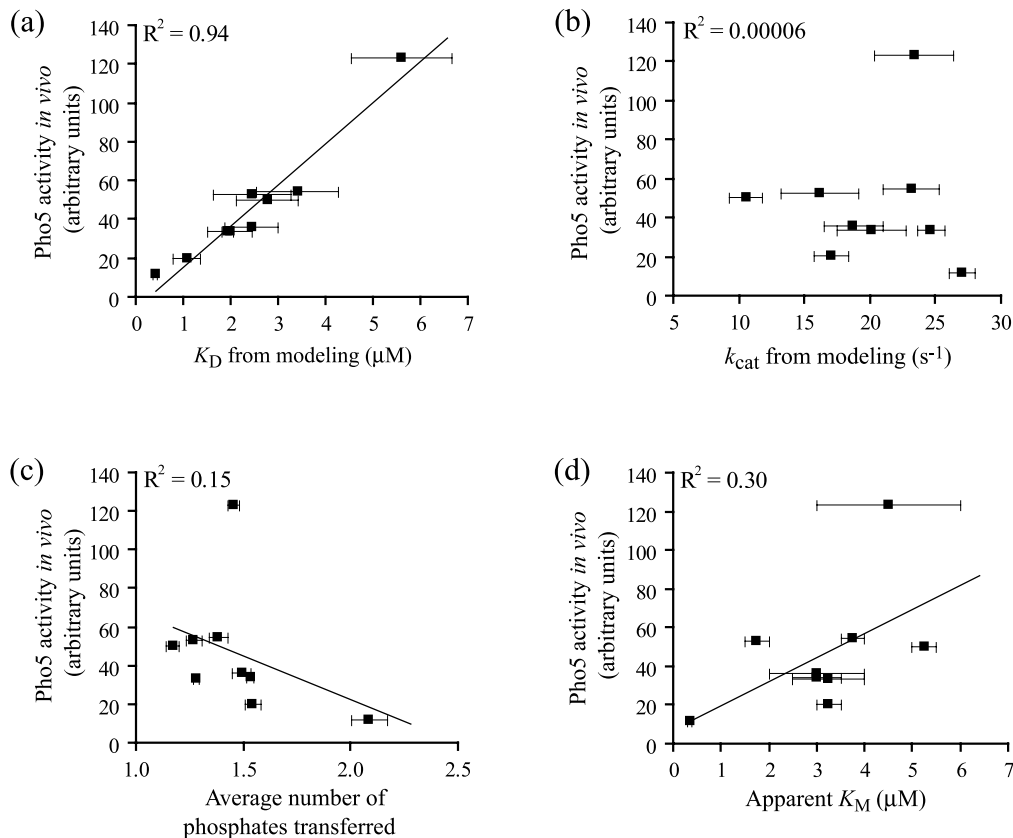


Figure 7. Testing the correlation between the relative *in vivo* $PHO4^C$ mutant phenotypes and *in vitro* kinetic parameters. (a) For wild-type $PHO4$ and each of the $PHO4^C$ mutants, Pho5 activity in cells grown in high-phosphate medium is compared to K_D for Pho80-Pho85 binding *in vitro*, as determined by computational modeling. The bars represent the range of K_D values obtained from the modeling that fit the data within error. (b) Pho5 activity of wild-type or mutant cells grown in high-phosphate medium is compared to k_{cat} , as determined by computational modeling. The bars represent the range of k_{cat} values obtained from the modeling that fit the data within error. (c) Pho5 activity of wild-type or mutant cells grown in high-phosphate medium is plotted against the number of times wild-type Pho4 or one of the Pho4 mutants is phosphorylated in a single binding event. The bars represent the range of values obtained from at least two independent experiments. (d) Pho5 activity of wild-type or mutant cells grown in high-phosphate medium is compared to apparent K_M values, which were calculated by fitting the experimental data to Lineweaver-Burk and Eadie-Hofstee plots. The bars represent the range of values obtained from at least two independent experiments.

led to an increase in the apparent K_M of the phosphorylation reaction but did not affect the apparent k_{cat} significantly. A similar result was obtained in a study investigating the kinetics of phosphorylation of a peptide derived from Cdc6, a substrate of cyclin A-CDK2 and cyclin E-CDK2.¹² This peptide contained a single phosphorylation site and a distal binding site containing a Cy motif. When the Cy motif was mutated, the K_M increased dramatically, but the k_{cat} was relatively unaffected. Thus, the distal binding site seems to be critical for increasing the affinity of the cyclin-CDK complex for its substrate, but does not significantly affect the rate of phosphotransfer.

We also investigated the effects of mutating the distal binding site on Pho4's multi-site phosphorylation and found that the $PHO4^C$ mutants were phosphorylated more distributively than wild-type. This result supports the idea that the distal binding site is important for controlling the processivity of

the phosphorylation reaction and suggests that the mutations alter the balance of k_{cat} to k_{off} that determines how many times Pho80-Pho85 phosphorylates Pho4 before dissociating from the substrate. This result has interesting implications for other multiply phosphorylated cyclin-CDK substrates such as Sic1 where the processivity of its phosphorylation would affect the ultrasensitivity and thus the timing of its destruction.²⁸

Finally, we fit the experimental data from the *in vitro* phosphorylation of the Pho4 mutants to a computational model that calculates the k_{on} , k_{off} , and k_{cat} values for phosphorylation of each of the five sites. The values for k_{on} and k_{off} derived from the modeling predict that the mutations decrease the binding affinity between Pho80-Pho85 and the Pho4 mutants. This supports the hypothesis that the mutations are located in a binding site that mediates a relatively high-affinity interaction with the kinase. Additionally, the predicted K_D

correlates well with Pho5 activity in wild-type and mutant cells grown in high-phosphate medium, suggesting that decreased binding at the distal, high-affinity site is an important determinant of the magnitude of the *in vivo* *PHO4^C* phenotype.

The correlation between the K_D values determined by the model and the *in vivo* level of Pho5 activity supports the validity of the model. In effect, the model is able to predict the increase in Pho5 activity *in vivo* by determining the K_D of the binding from the *in vitro* data. In addition, these results suggest that the data gathered *in vitro* are able to tell us something about the *in vivo* behavior. Of course, factors other than the kinase and substrate influence the phosphorylation reaction and Pho4 activity *in vivo*, including Pho81, Pho2, and a phosphatase that remains to be identified. Nevertheless these data suggest that the binding affinity between Pho80-Pho85 and Pho4, independent of other factors, plays an important role in Pho4 regulation, and that other factors in the cell may have a less significant influence on changing levels of Pho4 activity or may affect wild-type Pho4 and the Pho4 mutants in a similar way.

To our knowledge, the sequences corresponding to the cyclin-CDK-binding domains in Pho4 have not been identified in other kinase substrates. Neither of the two Pho80-binding domains in Pho4 contains the RXL motif found in distal binding sites of CDK2 substrates. Instead, the residues that are important in forming the distal binding site(s) in Pho4 are found in two distinct regions that have different amino acid sequences. We do not know if these two regions form one or two binding surfaces, because a complete structure of Pho4 or a Pho4 homologue is not available. Neither Pho81 nor any of the known or putative substrates of Pho85 contain sequences that are similar to those found in the two cyclin-CDK interacting domains in Pho4. It is possible that these sequences only mediate interactions between Pho80-Pho85 and its substrates, since Pho4 is the only known Pho80-Pho85 substrate.

A distal binding site is likely to be present in most cyclin-CDK substrates. The phosphorylation consensus sequence (S/TPXK/R) is common to most cyclin-CDK substrates and does not have enough variation to confer the specificity needed for different cyclin-CDK complexes to differentiate between substrates. Distal binding sites likely allow the cyclin components of the complexes, which have been identified as being important for substrate recognition, to target the substrate for phosphorylation by the CDK. However, it is still unclear exactly how distal binding sites in cyclin-CDK substrates help establish substrate specificity. In mammalian cells, it has been proposed that variation in the region surrounding the core Cy motif is responsible for increasing specificity. It is possible that different families of cyclin-CDKs target their substrates by recognizing different core binding motifs, just as Pho80-Pho85 recognizes a binding motif different from the Cy motif.

Furthermore, many cyclin-CDK substrates likely have distal binding sites to control processivity of phosphorylation and to modulate the overall efficiency of phosphorylation, both of which are potential mechanisms of substrate regulation.

Materials and Methods

Strains, plasmids, media, and general methods

The strains of *S. cerevisiae* used in this study are listed in Table 4,²⁹ and plasmids are listed in Table 5. Standard rich (YEPD) and synthetic (SD) media were used as described.³⁰ Phosphate-free and high-phosphate (11 mM potassium phosphate) media were made as described.³¹ Yeast cultures were grown at 30 °C for all experiments. Yeast transformations were performed by the lithium acetate method.³²

PCR mutagenesis and isolation of *PHO4^C* mutants

PCR mutagenesis was performed with 1.38 mM Mg²⁺ and 0.12 mM Mn²⁺ as described.³³ The primer pair

5'-GCAAATGAGTCTTGACC and

5'-CGGCGCGATTACTGCAGACTCACTTGCTAC

was used to amplify the first 684 bases of the *PHO4* open reading frame plus 110 bases of sequence upstream of the start codon. The PCR product was inserted into the plasmid EB0948, which is a YCp50³⁴ derivative containing the *PHO4* gene sequence encoding for amino acid residues 171–312, including a P224A mutation (PA6) and tagged with green fluorescent protein (GFP), all under the control of the *PHO4* promoter. In addition, a *NotI* endonuclease restriction site was introduced between the promoter and the gene sequence. The gel-purified PCR products and EB0948 that had been digested with *NotI* were co-transformed into a *pho4Δ pPHO5-HIS3* strain (EY0378). The transformed yeast cells were plated onto SD plates lacking histidine and uracil and containing 1 M sorbitol and 3 mM or 6 mM 3-amino-1,2,4-triazole. Cells that grew were retested using acid phosphatase plate assays, which identified Pho4 mutants that induce the expression of *PHO5* in cells grown on plates containing high-phosphate medium.³⁵ Plasmids were recovered from EY0378 and sequenced (ABI Prism).

Plasmid construction

Plasmids containing *PHO4^C* mutants were obtained as described above (see PCR mutagenesis and isolation of *PHO4^C* mutants). Most plasmids based on pAED4, a phage T7 RNA polymerase-based *E. coli* expression

Table 4. Strains of *S. cerevisiae* used in this study

Strain	Relevant genotype	Source or reference
K699	<i>MAT a ade2-1 trp1-1 can1-100 leu2-3,112 his3-11,15 ura3 GAL⁺</i>	29
EY0378	K699 <i>pho4::TRP1 his3::PHO5 pr-HIS3</i>	This work
EY0130	K699 <i>pho4::TRP1</i>	18
EY0219	K699 <i>pho4::TRP1 pho80::HIS3</i>	20
EY0270	K699 <i>pho4::TRP1 pho81::LEU2</i>	E.K.O. collection

Table 5. Plasmids used in this study

Plasmid	Relevant genotype	Source or reference
EB0948	pPHO4 pr-PHO4 ^{PA6} (a.a. 171–312)-GFP	This work
EB0127	pPHO4 pr-PHO4 in YCp50	18
EB1450	pPHO4 pr-PHO4-I22T in YCp50	This work
EB1451	pPHO4 pr-PHO4-L23H in YCp50	This work
EB1449	pPHO4 pr-PHO4-F29I in YCp50	This work
EB1452	pPHO4 pr-PHO4-L173S in YCp50	This work
EB1453	pPHO4 pr-PHO4-P174L in YCp50	This work
EB1454	pPHO4 pr-PHO4-D175V in YCp50	This work
EB1455	pPHO4 pr-PHO4-S176N in YCp50	This work
EB1491	pPHO4 pr-PHO4-L23H,P174L in YCp50	This work
EB0067	pT7 pr-PHO4 in pAED4	14
EB1257	pT7 pr-PHO4-I22T in pAED4	This work
EB1256	pT7 pr-PHO4-L23H in pAED4	This work
EB1447	pT7 pr-PHO4-F29I in pAED4	This work
EB1267	pT7 pr-PHO4-L173S in pAED4	This work
EB1277	pT7 pr-PHO4-P174L in pAED4	This work
EB1268	pT7 pr-PHO4-D175V in pAED4	This work
EB1269	pT7 pr-PHO4-S176N in pAED4	This work
EB1467	pT7 pr-PHO4-L23H,P174L in pAED4	This work
EB1164	pT7 pr-PHO85-His ₆ in pQE-60	21
EB1076	pT7 pr-PHO80 in pSBETA	21
EB0486	pPHO4 pr-PHO4-GFP in pRS315	E.K.O. collection

vector,³⁶ and containing PHO4^C mutants were constructed by cloning *BsmI*-*MluI* fragments from the original PHO4^C mutant-containing plasmids into the *BsmI* and *MluI* sites of EB0067. EB1447 was generated by performing site-directed mutagenesis on EB0067.³⁷ EB1277 was generated by cloning the *BsmI*-*MluI* fragment from EB1274 into the *BsmI* and *MluI* sites of EB0067. Vectors for expression in yeast are based on YCp50,³⁴ a low-copy-number *CEN-ARS E. coli-S. cerevisiae* shuttle vector. Most vectors based on YCp50 were constructed by cloning *HindIII*-*MluI* fragments from the original PHO4^C mutant-containing plasmids into the *HindIII* and *MluI* sites of EB0127. EB1449 was generated by cloning the *BsmI*-*MluI* fragment from EB1447 into the *BsmI* and *MluI* sites of EB0486, then cloning the *HindIII*-*MluI* fragment from that plasmid into the *HindIII* and *MluI* sites of EB0127. All plasmids containing PCR products and single-site mutations in the PHO4 gene were confirmed by sequencing analysis (ABI Prism).

Liquid acid-phosphatase assays

The strains *pho4Δ* (EY0130), *pho4Δ pho80Δ* (EY0219), and *pho4Δ pho81Δ* (EY0270) were freshly transformed with YCp50 or with YCp50-based plasmids containing pPHO4pr-PHO4 or pPHO4pr-PHO4 with each of the PHO4^C single-site mutations. Cells were grown overnight to mid-log phase in SD-Uracil. Then, they were washed three times with high-phosphate or phosphate-free medium before being resuspended to an A_{600} of 0.2 in high-phosphate medium or 0.25 in phosphate-free medium. The cells were then grown for three hours at 30 °C. Pho5 activity was assessed by a liquid acid phosphatase assay, which measures the activity of secreted acid phosphatase by determining the amount of *p*-nitrophenylphosphate cleaved during a ten minute incubation at room temperature versus cell-culture density. The amount of *p*-nitrophenyl was determined spectrophotometrically at 420 nm (A_{420}) and cell-culture density was determined at 600 nm (A_{600}). The assay was performed essentially as described³⁵ but with the follow-

ing modifications: the reaction mix contained 5.6 mg/ml of *p*-nitrophenylphosphate and 0.1 M acetate buffer (pH 4.2).

Protein expression and purification

Msn5-His₆ was expressed in *E. coli* and purified using a Hi-Trap chelating column loaded with NiSO₄ as described.²⁷ RanQ69L with an N-terminal zz tag was expressed in *E. coli* (strain SG13009). Bacterial cells containing the zz-RanQ69L expression vector (EB810) were grown in LB with 100 μg/ml of carbenicillin and 25 μg/ml of kanamycin to an A_{600} of 0.6 and expression was induced with 1 mM IPTG for four hours at room temperature. Cells were resuspended in IgG buffer (50 mM Tris-HCl (pH 7.5), 150 mM NaCl, 0.05% (v/v) Tween 20, 5 mM MgCl₂, 1 mM β-mercaptoethanol) containing 10% (v/v) glycerol, 5 μM GTP, and protease inhibitors (1 mM phenylmethylsulfonyl fluoride (PMSF), 2 mM benzamide, 1 μg/ml of leupeptin, 1 μg/ml of pepstatin); lysed by sonication; and cleared by centrifugation at 100,000g in a Beckman Ti60 rotor for one hour at 4 °C. Lysate was stored in aliquots at -80 °C. GST-Pho85-Pho80 was purified using glutathione (GSH)-agarose (Sigma) as described.³¹ Pho4 wild-type and mutant proteins were expressed in *E. coli* and purified using ion-exchange chromatography as described.¹⁴ Pho4 proteins were purified using an Akta Explorer 10 FPLC (Amersham Pharmacia). Pho80-Pho85-His₆ was expressed in *E. coli* and purified using a 1 ml Hi-Trap chelating column (Pharmacia) loaded with NiSO₄ as described.²¹ Pho4 and Pho80-Pho85-His₆ concentrations were measured by recording absorbance at 280 nm in 6 M guanidinium HCl at pH 6.5.³⁸ The purity of the Pho4 protein preparations and the Pho80-Pho85 complex was estimated to be >95% by SDS-PAGE and staining with Coomassie brilliant blue. The identity of wild-type Pho4 and the Pho4 mutants was confirmed by electrospray mass spectrometry, which indicates that the N-terminal methionine residue is cleaved off all the Pho4 proteins, as expected.¹⁴

Binding assay with Msn5 and RanGTP

Wild-type and mutant Pho4 were phosphorylated to completion by incubating 15 μM Pho4 with 100 nM Pho80-Pho85-His₆, 0.34 μM [γ -³²P]ATP (Amersham, 6000 Ci mM⁻¹), 0.72 mM ATP, and kinase buffer (20 mM Tris-HCl (pH 7.5), 10 mM MgCl₂) in IgG buffer plus 10% glycerol and protease and phosphatase inhibitors (1 mM PMSF, 2 mM benzamide, 1 μg/ml of leupeptin, 1 μg/ml of pepstatin, and 20 nM calyculin A) for 20 minutes at 30 °C. Phosphorylated protein was separated from unincorporated ATP on Bio-Spin 6 columns (Bio-Rad) equilibrated with IgG buffer plus 10% glycerol and inhibitors. The same reaction without [γ -³²P]ATP was performed to phosphorylate Pho4 for binding assays analyzed by Western blotting. Aliquots of phosphorylated Pho4 were frozen at -80 °C. Phosphorylated Pho4 was analyzed on an isoelectric-focusing gel to confirm that phosphorylation was complete. To purify zz-RanQ69L, saturating amounts of bacterial lysate containing zz-RanQ69L were bound to 25 μl of IgG-Sepharose by incubating at 4 °C for one hour. The resin with bound zz-RanQ69L was washed with IgG buffer plus inhibitors and 100 μM GTP and re-equilibrated with IgG buffer plus inhibitors. Immobilized zz-RanQ69L was incubated for one hour at room

temperature with Msn5-His₆ (50, 100, 300, 500, or 700 nM), 100 nM phosphorylated wild-type or mutant Pho4, and 160 μg BSA. The resin was washed extensively with IgG buffer and bound proteins were eluted with boiling 2 × sample buffer (³²P-labeled sample) or with IgG buffer containing 1 M MgCl₂ and concentrated by precipitation in methanol/chloroform (Western blot). Quantification was done using a Phosphorimager (Molecular Dynamics) and Image Quant software (version 5.2, Molecular Dynamics).

Binding assay with GST-Pho85-Pho80

Wild-type and mutant Pho4 were transcribed and translated *in vitro* in the presence of [³⁵S]methionine using rabbit reticulocyte lysate at 30 °C for 90 minutes according to the manufacturer's protocol (Promega TNT kit). Protein was frozen in aliquots at -80 °C. For the binding reactions, 400, 62.5, 25, 10, or 4 nM GST-Pho85-Pho80 was incubated with GSH-agarose equilibrated in binding buffer (50 mM Tris-HCl (pH 7.5), 150 mM NaCl, 0.05% Tween 20, 5 mM MgCl₂, 1 mM β-mercaptoethanol, 1 mM PMSF, 2 mM benzamidine, 1 μg/ml of leupeptin, 1 μg/ml of pepstatin) for two hours at 4 °C. GST-Pho85 at 4 nM and 400 nM was used as a negative binding control. The resin was washed twice with binding buffer and once with binding buffer plus 10% glycerol. Then, 0.2 nM ³⁵S-labeled Pho4 was incubated with the bound GST-Pho85-Pho80 for one hour at room temperature, and the resin was washed extensively and pelleted. Pellets were resuspended in 2 × SDS sample buffer, boiled, and separated by SDS-PAGE. Analysis of bound Pho4 was performed using a Phosphorimager (Molecular Dynamics).

Production of anti-phospho-Pho4 antibodies

Anti-phospho-SP2, anti-phospho-SP3, and anti-phospho-SP6 antibodies were made by Bethyl Laboratories, Inc (Montgomery, TX). Rabbit polyclonal anti-phospho-SP2, anti-phospho-SP3, and anti-phospho-SP6 were raised against peptides containing phospho-SP2 (CPRLYS(-PO₄)PLIHT), phospho-SP3 (VPVTIS(-PO₄)PNLVACG), phospho-SP6 (VVASES(-PO₄)PVIAPCG). Antibodies reactive with non-phosphorylated peptide were removed by absorption on an immunoabsorbent containing non-phosphorylated peptide. The antibodies were then affinity-purified using a column charged with the antigen peptide. The three antibodies do not react significantly in Western blots with recombinant, unphosphorylated Pho4 (data not shown) or Pho4 in cell extracts made from *pho80Δ* cells, where Pho4 is not phosphorylated (Figure 4(b)).

Preparation of cell extracts and Western blotting

Cells were first grown to an A₆₀₀ of 0.6–1.0 in SD medium supplemented with amino acids. Overnight cultures were diluted and grown to an A₆₀₀ of 0.3–0.4. Approximately 5.7 × 10⁷–6.0 × 10⁷ cells were pelleted, frozen in liquid nitrogen, and stored at -80 °C. For cell lysis, 100 μl of boiling 2 × SDS protein sample buffer (20% (v/v) glycerol, 125 mM Tris-HCl (pH 6.8), 6% (w/v) SDS, 10% (v/v) β-mercaptoethanol, 0.001% (w/v) bromophenol blue, 2 mM PMSF, 2.5 mM benzamidine, 1 μg/ml of leupeptin, 1 μg/ml of pepstatin, 80 mM β-glycerophosphate, 10 mM NaF, 20 nM calyculin A) was added to the frozen cell pellets, followed by 150–

200 μl of acid-washed glass beads. Cell pellets were heated at 100 °C for two minutes, vortexed for one minute, then heated at 100 °C for two minutes. The supernatants were diluted with 100 μl of high-salt buffer (20 mM Tris-HCl (pH 7.5), 0.5 M NaCl, 0.05% (v/v) NP-40, 1 mM EDTA, 10% (v/v) glycerol, 2 mM PMSF, 2.5 mM benzamidine, 1 μg/ml of leupeptin, 1 μg/ml of pepstatin, 80 mM β-glycerophosphate, 10 mM NaF, 20 nM calyculin A). The lysates were spun twice in a microfuge for five minutes at 4 °C. Cell extract (20 μl) was loaded onto a 7.8% (w/v) polyacrylamide gel and analyzed by SDS-PAGE, followed by Western blotting. In the Western blotting analysis, primary antibody was followed by a secondary goat anti-rabbit antibody conjugated to horseradish peroxidase and immunoreactive proteins were visualized using a chemiluminescent substrate. The chemiluminescent signal was detected using an AlphaImager CCD camera (Alpha Innotech) and analyzed using AlphaEaseFC software (Alpha Innotech).

Kinase assays

Phosphate transfer to Pho4 by Pho80-Pho85 was measured using kinase assays as described.²¹ The kinase assays used to measure molar phosphate transferred by Pho80-Pho85 at a single Pho4 concentration contained 1 μM Pho4 and 0.1 nM Pho80-Pho85. The kinase reactions used to measure the apparent *k*_{cat} and *K*_M were performed with 1 nM Pho80-Pho85 (Pho4 mutants) or 0.1 nM Pho80-Pho85 (wild-type Pho4), eight different concentrations of Pho4 surrounding the *K*_M, 85 nM [γ -³²P]ATP (Amersham; 6000 Ci mM⁻¹), and 900 μM ATP. All reactions used to measure the rate of phosphate transfer were stopped by the addition of 2 × SDS-PAGE sample buffer and separated by 12% SDS-PAGE. Apparent *k*_{cat} and *K*_M were determined from Lineweaver–Burk and Eadie–Hofstee plots. We calculated *k*_{cat} from *V*_{max} assuming 100% activity of the enzyme. Kinase reactions used to measure early phosphoform production contained 0.2 nM Pho80-Pho85, 6 μM Pho4, 170 nM [γ -³²P]ATP (Amersham; 6000 Ci mM⁻¹), and 450 μM ATP. The reactions were stopped by the addition of EDTA (50 mM final concentration) and frozen immediately with liquid nitrogen. The reactions were then run on IEF gels. All quantification was done using a Phosphorimager (Molecular Dynamics) and Image Quant software (version 5.2, Molecular Dynamics).

Isoelectric focusing gels

The five phosphoforms of Pho4 were separated on the basis of their isoelectric points (pI) by IEF gels as described.²¹ A single experiment to determine the processivity of phosphoform production included 12–18 time-points. The distribution of phosphoforms was determined as a fraction of the total phosphorylated Pho4 at each time-point.

Computational modeling

The data from the *in vitro* phosphorylation of wild-type and mutant Pho4 was fit to the constant *k*_{on}, variable *k*_{off}, decreasing *k*_{cat} model of the Pho4 phosphorylation reaction as described.²¹ The model was modified slightly to fit the relative phosphoforms at low kinase and high substrate concentration (0.1 nM and 6 μM, respectively) rather than the time-course of phosphoform production (2 nM kinase, 3 μM substrate). The experimental data

for wild-type Pho4 published previously was refit to the modified model and the predicted kinetic constants were the same within error.²¹ We used a multi-variable, random-walk search and least-squares analysis to find the best-fit values. All variables were fit to a level where they are statistically indistinguishable from the experimental data at least 95% of the time.

Acknowledgements

We thank members of the O'Shea laboratory for critical reading of the manuscript and David King for the mass spectrometry analysis. This work was supported by grants from the N.I.H. (GM51377), the David and Lucile Packard Foundation (to E.K.O.), and the Howard Hughes Medical Institute (to E.K.O.). M.B. is supported by a pre-doctoral fellowship from the National Science Foundation. M.S. is supported by a pre-doctoral fellowship from the Burroughs Wellcome Foundation.

References

1. Carroll, A. S. & O'Shea, E. K. (2002). Pho85 and signaling environmental conditions. *Trends Biochem. Sci.* **27**, 87–93.
2. Morgan, D. O. (1997). Cyclin-dependent kinases: engines, clocks, and microprocessors. *Annu. Rev. Cell Dev. Biol.* **13**, 261–291.
3. Brown, N. R., Noble, M. E., Endicott, J. A. & Johnson, L. N. (1999). The structural basis for specificity of substrate and recruitment peptides for cyclin-dependent kinases. *Nature Cell Biol.* **1**, 438–443.
4. Moffat, J., Huang, D. & Andrews, B. (2000). Functions of Pho85 cyclin-dependent kinases in budding yeast. *Prog. Cell Cycle Res.* **4**, 97–106.
5. Roberts, J. M. (1999). Evolving ideas about cyclins. *Cell*, **98**, 129–132.
6. Songyang, Z., Blechner, S., Hoagland, N., Hoekstra, M. F., Pivnicka-Worms, H. & Cantley, L. C. (1994). Use of an oriented peptide library to determine the optimal substrates of protein kinases. *Curr. Biol.* **4**, 973–982.
7. Holmes, J. K. & Solomon, M. J. (1996). A predictive scale for evaluating cyclin-dependent kinase substrates. A comparison of p34cdc2 and p33cdk2. *J. Biol. Chem.* **271**, 25240–25246.
8. Schulman, B. A., Lindstrom, D. L. & Harlow, E. (1998). Substrate recruitment to cyclin-dependent kinase 2 by a multipurpose docking site on cyclin A. *Proc. Natl Acad. Sci. USA*, **95**, 10453–10458.
9. Adams, P. D., Li, X., Sellers, W. R., Baker, K. B., Leng, X., Harper, J. W. *et al.* (1999). Retinoblastoma protein contains a C-terminal motif that targets it for phosphorylation by cyclin-cdk complexes. *Mol. Cell. Biol.* **19**, 1068–1080.
10. Adams, P. D., Sellers, W. R., Sharma, S. K., Wu, A. D., Nalin, C. M. & Kaelin, W. G., Jr (1996). Identification of a cyclin-cdk2 recognition motif present in substrates and p21-like cyclin-dependent kinase inhibitors. *Mol. Cell. Biol.* **16**, 6623–6633.
11. Petersen, B. O., Lukas, J., Sorensen, C. S., Bartek, J. & Helin, K. (1999). Phosphorylation of mammalian CDC6 by cyclin A/CDK2 regulates its subcellular localization. *EMBO J.* **18**, 396–410.
12. Takeda, D. Y., Wohlschlegel, J. A. & Dutta, A. (2001). A bipartite substrate recognition motif for cyclin-dependent kinases. *J. Biol. Chem.* **276**, 1993–1997.
13. Lowe, E. D., Tews, I., Cheng, K. Y., Brown, N. R., Gul, S., Noble, M. E. *et al.* (2002). Specificity determinants of recruitment peptides bound to phospho-CDK2/Cyclin A. *Biochemistry*, **41**, 15625–15634.
14. Kaffman, A., Herskowitz, I., Tjian, R. & O'Shea, E. K. (1994). Phosphorylation of the transcription factor PHO4 by a cyclin-CDK complex, PHO80-PHO85. *Science*, **263**, 1153–1156.
15. Oshima, Y. (1997). The phosphatase system in *Saccharomyces cerevisiae*. *Genes Genet. Syst.* **72**, 323–334.
16. Schneider, K. R., Smith, R. L. & O'Shea, E. K. (1994). Phosphate-regulated inactivation of the kinase PHO80-PHO85 by the CDK inhibitor PHO81. *Science*, **266**, 122–126.
17. Ogawa, N., DeRisi, J. & Brown, P. O. (2000). New components of a system for phosphate accumulation and polyphosphate metabolism in *Saccharomyces cerevisiae* revealed by genomic expression analysis. *Mol. Biol. Cell*, **11**, 4309–4321.
18. O'Neill, E. M., Kaffman, A., Jolly, E. R. & O'Shea, E. K. (1996). Regulation of PHO4 nuclear localization by the PHO80-PHO85 cyclin-CDK complex. *Science*, **271**, 209–212.
19. Komeili, A. & O'Shea, E. K. (1999). Roles of phosphorylation sites in regulating activity of the transcription factor Pho4. *Science*, **284**, 977–980.
20. Kaffman, A., Rank, N. M. & O'Shea, E. K. (1998). Phosphorylation regulates association of the transcription factor Pho4 with its import receptor Pse1/Kap121. *Genes Dev.* **12**, 2673–2683.
21. Jeffery, D. A., Springer, M., King, D. S. & O'Shea, E. K. (2001). Multi-site phosphorylation of Pho4 by the cyclin-CDK Pho80-Pho85 is semi-processive with site preference. *J. Mol. Biol.* **306**, 997–1010.
22. Huang, D., Moffat, J., Wilson, W. A., Moore, L., Cheng, C., Roach, P. J. & Andrews, B. (1998). Cyclin partners determine Pho85 protein kinase substrate specificity *in vitro* and *in vivo*: control of glycogen biosynthesis by Pcl8 and Pcl10. *Mol. Cell. Biol.* **18**, 3289–3299.
23. Jayaraman, P. S., Hirst, K. & Goding, C. R. (1994). The activation domain of a basic helix-loop-helix protein is masked by repressor interaction with domains distinct from that required for transcription regulation. *EMBO J.* **13**, 2192–2199.
24. Okada, H. & Toh-e, A. (1992). A novel mutation occurring in the PHO80 gene suppresses the PHO4^c mutations of *Saccharomyces cerevisiae*. *Curr. Genet.* **21**, 95–99.
25. Ogawa, N. & Oshima, Y. (1990). Functional domains of a positive regulatory protein, PHO4, for transcriptional control of the phosphatase regulon in *Saccharomyces cerevisiae*. *Mol. Cell. Biol.* **10**, 2224–2236.
26. Bischoff, F. R., Klebe, C., Kretschmer, J., Wittinghofer, A. & Ponstingl, H. (1994). RanGAP1 induces GTPase activity of nuclear Ras-related Ran. *Proc. Natl Acad. Sci. USA*, **91**, 2587–2591.
27. Kaffman, A., Rank, N. M., O'Neill, E. M., Huang, L. S. & O'Shea, E. K. (1998). The receptor Msn5 exports the phosphorylated transcription factor Pho4 out of the nucleus. *Nature*, **396**, 482–486.
28. Nash, P., Tang, X., Orlicky, S., Chen, Q., Gertler, F. B., Mendenhall, M. D. *et al.* (2001). Multisite phos-

- phorylation of a CDK inhibitor sets a threshold for the onset of DNA replication. *Nature*, **414**, 514–521.
29. Nasmyth, K., Adolf, G., Lydall, D. & Seddon, A. (1990). The identification of a second cell cycle control on the HO promoter in yeast: cell cycle regulation of SW15 nuclear entry. *Cell*, **62**, 631–647.
 30. Sherman, F. (1991). Getting started with yeast. *Methods Enzymol.* **194**, 3–21.
 31. Huang, S., Jeffery, D. A., Anthony, M. D. & O'Shea, E. K. (2001). Functional analysis of the cyclin-dependent kinase inhibitor Pho81 identifies a novel inhibitory domain. *Mol. Cell. Biol.* **21**, 6695–6705.
 32. Guthrie, C. & Fink, G. R. (1991). Editors of *Guide to Yeast Genetics and Molecular Biology*, vol. 194, Academic Press, San Diego, CA.
 33. Leung, D. W., Chen, E. Y. & Goeddel, D. V. (1989). A method for random mutagenesis of a defined DNA segment using a polymerase chain reaction. *Technique*, **1**, 11–15.
 34. Johnston, M. & Davis, R. W. (1984). Sequences that regulate the divergent GAL1-GAL10 promoter in *Saccharomyces cerevisiae*. *Mol. Cell. Biol.* **4**, 1440–1448.
 35. Toh-e, A., Ueda, Y., Kakimoto, S. I. & Oshima, Y. (1973). Isolation and characterization of acid phosphatase mutants in *Saccharomyces cerevisiae*. *J. Bacteriol.* **113**, 727–738.
 36. Doering, D. (1992). Functional and structural studies of a small f-actin binding protein. PhD thesis. Massachusetts Institute of Technology.
 37. Kunkel, T. A., Roberts, J. D. & Zakour, R. A. (1987). Rapid and efficient site-specific mutagenesis without phenotypic selection. *Methods Enzymol.* **154**, 367–382.
 38. Edelhoch, H. (1967). Spectroscopic determination of tryptophan and tyrosine in proteins. *Biochemistry*, **6**, 1948–1954.
 39. McAndrew, P. C., Svaren, J., Martin, S. R., Horz, W. & Goding, C. R. (1998). Requirements for chromatin modulation and transcription activation by the Pho4 acidic activation domain. *Mol. Cell. Biol.* **18**, 5818–5827.

Edited by S. Reed

(Received 12 May 2003; received in revised form 13 October 2003; accepted 13 October 2003)